JOURNAL OF SPACECRAFT AND ROCKETS
Vol. 40, No. 1, January–February 2003

Mach 10 Hypersonic Nozzle: Improved Flow Quality

John Lacey*
Aero Systems Engineering, St. Paul, Minnesota 55107
Yasutoshi Inoue†
National Aerospace Laboratory, Tokyo 182-8522, Japan
Akio Higashida‡
Mitsubishi Heavy Industries, Ltd., Kobe 652-8585, Japan
Manabu Inoue§
Mitsubishi Heavy Industries, Ltd., Tokyo 100-8315, Japan
Kouichi Ishizaka¶
Mitsubishi Heavy Industries, Ltd., Takasago Hyogo 676-8686, Japan
and
John J. Korte**
NASA Langley Research Center, Hampton, Virginia 23681

The flow quality of the Mach 10 nozzle (exit diameter 1.27 m) at the National Aerospace Laboratory, Chofu, has been significantly improved. The spread of pitot pressure ratio over nearly 60% of the test section width and height was reduced from ±7.5 to ±1.5%. This was accomplished by remachining the nozzle based on a new technique for smoothing the method of characteristics plus boundary-layer correction coordinates. Various sets of possible smoothed contours were checked using two computational fluid dynamics (CFD) codes before selecting one set for machining. These codes were run with the initial contour, and the CFD results were validated by comparison to the initial test data before checking the suggested contours. The change in nozzle radius was less than 1 mm.

Nomenclature

Grad P	=	$[(dP/dX)^2 + (dP/dR)^2]^{0.5}$
P	=	nondimensionalized pressure, p/p_0
p	=	static pressure, Pa
p_0, p_{t1}	=	upstream total pressure, Pa
p_{t2}	=	total pressure behind normal shock in test section, Pa
R	=	nondimensionalized coordinate in the radial direction, r/r^*
r	=	nozzle coordinate in the radial direction, mm
r^*	=	throat radius, 24.182 mm
X	=	nondimensionalized coordinate in the longitudinal direction, x/r^*
x	=	nozzle coordinate in the longitudinal direction, mm; axial location of pitot rake from the end of the test section, mm
z	=	vertical location of pitot rake from test section centerline, mm

Received 25 January 2002; revision received 2 September 2002; accepted for publication 25 September 2002.

*Wind Tunnel Marketing, Department of Marketing, 358 East Fillmore Avenue; jlacey@aerosysengr.com. Member AIAA.
†Director, Department of Fluid Science Research, 7-44-1 Jindaiji-Hidushi-Machi, Chofu City; yinoue@nal.go.jp. Senior Member AIAA.
‡Manager, Machinery and Space Systems Department, Kobe Shipyard and Machinery Works, 1-1 Wadasaki-Cho 1-Chome, Hyogo-Ku; akio-higashida@kind.kobe.mhi.co.jp.
§Acting Manager, Turbomachinery and General Machinery Department, Machinery Headquarters, 5-1 Marunouchi 2-Chome, Chiyoda-Ku; manabu_inoue@hq.mhi.co.jp.
¶Senior Research Engineer, Turbomachinery Laboratory, Takasago Research and Development Center, 2-1-1 Shinhama Arai-Cho; ishizaka@wb.trdc.mhi.co.jp.
**Senior Research Engineer, Mail Stop 159, Multi-Discipline Optimization Department; j.j.korte@larc.nasa.gov. Associate Fellow AIAA.

Introduction

THE 1.27-m-diam Mach 10 nozzle at the National Aerospace Laboratory (NAL) at Chofu, Japan, was designed in the early 1990s for a nominal design point of 1070 K and 6 MPa. This nozzle was designed and manufactured in accordance with industry standards at the time. The flow quality (Fig. 1) of this project was acceptable at the time as compared to other tunnels[1]; however, since then wind tunnels with better performance have been offered.[2] The tighter tolerance limits used by the industry can be inferred from Refs. 3 and 4, where the resolution in Mach number changed from 0.20 to 0.01, respectively. As a result, the Chofu design was not satisfactory compared to the current world-class performance criteria.[5]

The purpose of this effort was to improve the flow quality of the NAL Chofu Mach 10 facility up to the state of the art for hypersonic testing. Only with such an improvement will test data from the facility be comparable to those of others around the world. The improved quality is also necessary to allow use of larger models in the entire test section.

Other researchers have investigated similar problems,[6,7] and the present effort is seen as another example of a detailed investigation to improve flow quality of hypersonic nozzles. The program described herein was initiated to improve the flow quality through the following steps: 1) computational fluid dynamics (CFD) modeling of the existing flow, 2) development of possible nozzle contours, 3) evaluation of these nozzle contours, 4) remachining of the nozzle, and 5) validation testing.

Mitsubishi Heavy Industries (MHI), Aero Systems Engineering (ASE), and NASA Langley Research Center (LaRC) participated in this effort with NAL. Researchers at NAL obtained experimental data and analyzed the flow characteristics in detail; they also determined the overall specification and provided project management of the program. Investigators at MHI did the contour measurements and the remachining. Participants at MHI and NASA LaRC used their CFD capability to model the original test results and to evaluate the new contours. Associates at ASE collaborated to develop the improved nozzle contours.

Analysis: Existing Contour

As shown in Fig. 2, the detailed experimental data indicate pressure waves traversing the test section and the effects of other waves

converging on the centerline. The profile was shown to be nearly symmetrical. The spread of pitot pressure ratio is shown to be ±7.5%; this spread of pitot pressure implies a Mach number variation of ±1.4%. (All test data in this paper are at the nominal design point of 6 MPa total pressure, 1070 K total temperature, and $M \sim 10$.)

Through a preliminary CFD analysis these waves were speculated to originate from the nozzle wall as shown in Fig. 3. Whereas one wave could come from the joint between expansion 1 and expansion 2, the others were not so obvious. Those other waves could be reflections of waves that originated farther upstream, or they could be waves generated on the nozzle wall at the location shown. Therefore, the wall contour was precisely measured at many stations so that small disturbances could be detected. The results of these measurements showed that the contour was, in general, typical of hypersonic nozzles, but the slope and curvature were not fully smooth, as shown in Fig. 4 for the throat and initial expansion.

The complete measured contour data were placed in the CFD codes of both LaRC and MHI, and the predictions are shown in Figs. 5 and 6, respectively. In each case, the general character of the nonuniform profiles is predicted. (The differences that do exist are not deemed to be significant because a prediction of such steep gradients is subject to exact measurements of all peaks and valleys. Although the coordinates of the contour were measured in fine detail, there is the possibility that some peaks/valleys were not recorded and/or that some gas properties are not fully modeled.)

The following points briefly describe the MHI CFD method: 1) three stage Runge–Kutta scheme, 2) flux vector splitting compact total variation diminishing (fifth-order),[8] 3) Baldwin–Barth turbulence model (one-equation model), and 4) gas properties based on Refs. 9 and 10. The code used 401 points in the axial direction and 71 in the radial direction. The code is more fully described in Ref. 8.

The NASA LaRC method uses the CANDO code that is described in Ref. 11 and has proven applications in Refs. 12 and 13. To calculate the nozzle flowfield, the nozzle is divided into two regions: the subsonic–transonic section and the supersonic–hypersonic section. In the subsonic–transonic section, the full Navier–Stokes (NS) equations are solved. In the supersonic–hypersonic section, the

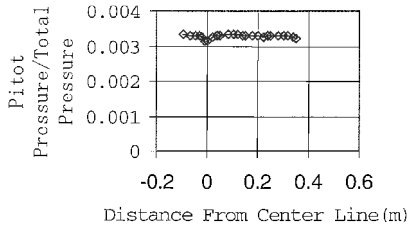

Fig. 1 Pitot pressure distributions at design point profile; center of the test section.

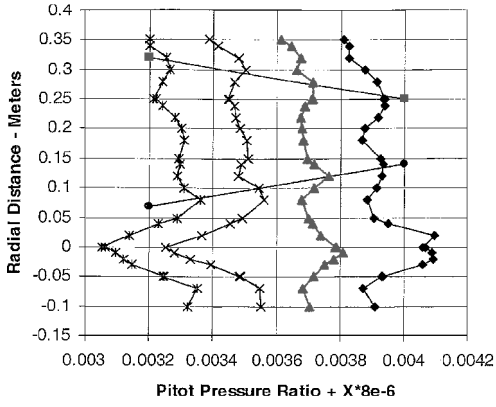

Fig. 2 Pitot pressure profiles, various axial stations X: ◆, 75 cm; ▲, 50 cm; ×, 25 cm; ∗, 0 cm; ■ and ●, Mach 10.

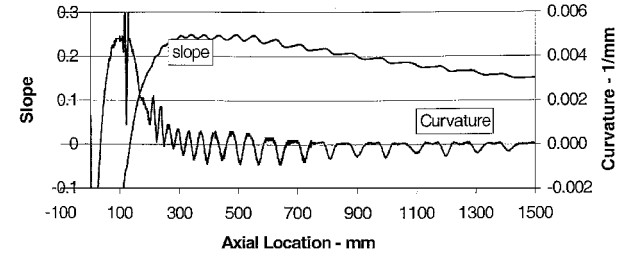

Fig. 4 Original slope and curvature.

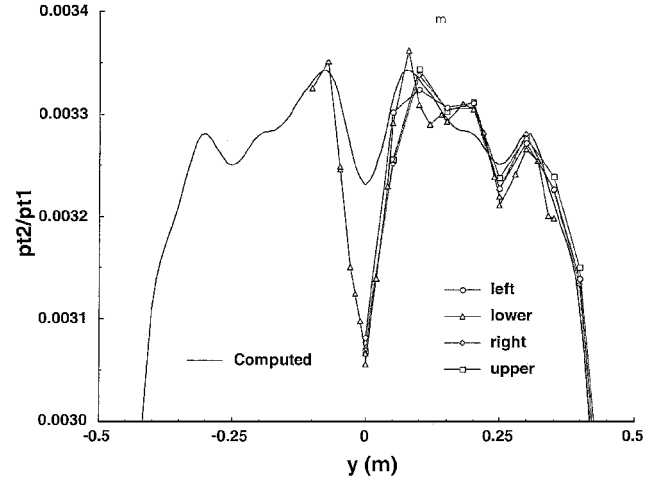

Fig. 5 Comparisons of pitot pressure profiles with CFD, NASA LaRC.

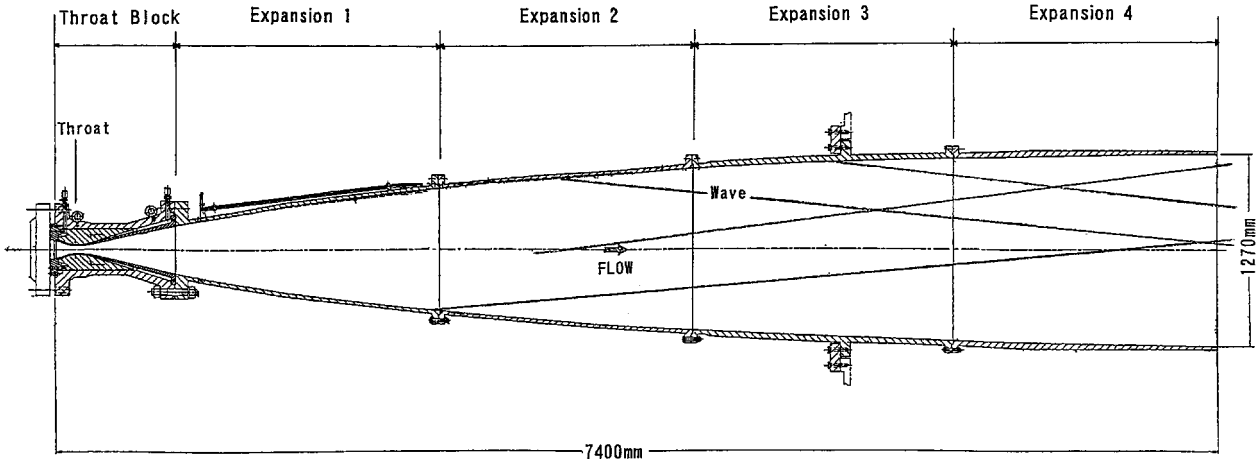

Fig. 3 Nozzle sections and possible wave pattern.

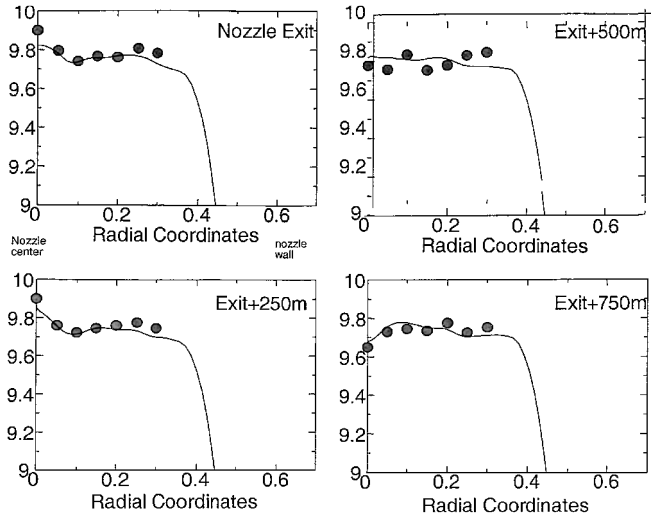

Fig. 6 Comparisons of Mach number profiles with CFD, MHI: ●, measurement and ——, CFD prediction.

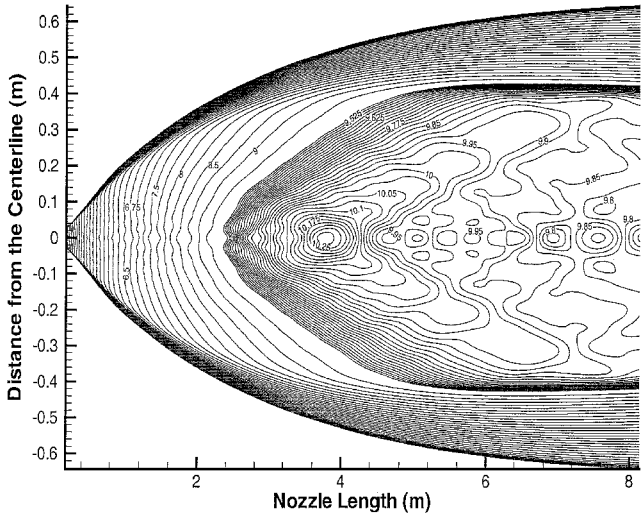

Fig. 7 Typical Mach contour.

parabolized NS equations are solved. The subsonic–transonic grid was 75 × 125 points in the axial and normal directions, respectively. The centerline Mach number started at approximately 0.2 and ended at a 1.8 Mach number for the first region. The downstream calculations started at approximately 1.4 Mach number and took approximately 1×10^6 space marching steps. The numerical grid stretching was controlled to maintain $y+ < 5$.

Other Tools for Analysis

Along with the pitot pressure profiles, the usual contour maps of Mach, pressure, velocity, etc., were also obtained. (See Fig. 7 for an example.) The origins of waves were not easily interpreted from these usual contour plots. Therefore, the parameter Grad P/P was developed. This parameter is not dependent on the selection of resolution, as was required for the contours in Fig. 7. These contours are shown in Fig. 8 for the original nozzle, and they depict gradients in the flow in all parts of the nozzle. The many waves that come from the wall can be seen, and some of these traverse the test section. Strong gradients on the centerline are also obvious in Fig. 8. Two waves generally agree with the two pressure waves that were identified in Fig. 2. The agreement between experimental data and CFD predictions validated the use of CFD to predict flow quality of a revised contour.

Contour Smoothing

Initial Smoothing

Based on the successful validation of the CFD models, new contours were developed in an attempt to obtain a more uniform flow.

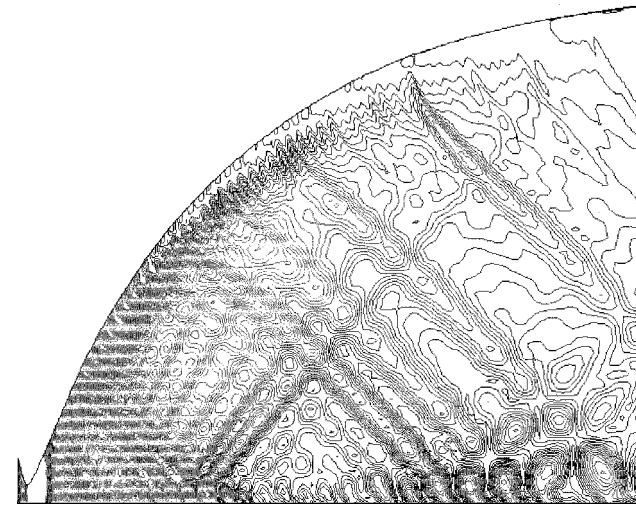

Fig. 8 Contour of Grad *P/P* for original nozzle.

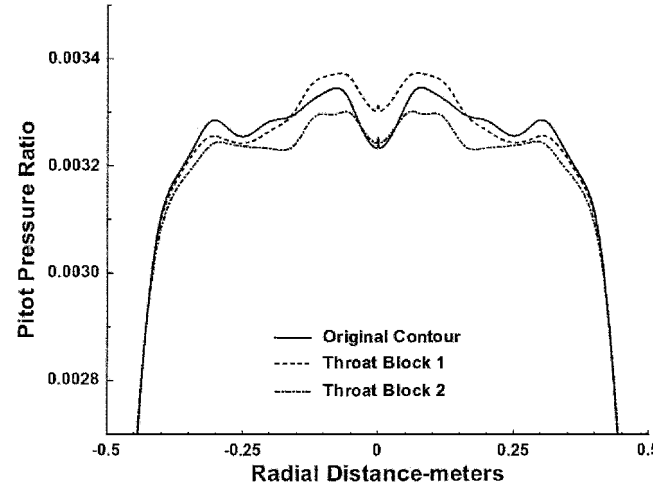

Fig. 9 Pitot pressure profile for two cases of throat block smoothing.

One criterion for these new contours was that the existing nozzle (except the throat block) had to be reused to minimize cost.

The first attempt was to smooth just the throat block, that is, the initial expansion of the nozzle. The nozzle block is a small section and could be remade for relatively low cost. The results are shown in Fig. 9. Note that in both cases that were studied, major nonuniformities still remain. Thus, it does not seem possible to achieve uniform flow with modification of only the throat block. Further attempts to obtain uniform flow considered the entire nozzle, not just the throat block.

Final Smoothing

The original contour was based on the method of characteristics plus boundary-layer correction (MOC + BL) and was then smoothed using cubic spline methods. For the new coordinates, a revised smoothing method was used based on polynomial equations of the nozzle radius as a function of the nozzle axial location. The nozzle was divided into axial sections for the curve fit procedure. To avoid sudden changes of slope in the nozzle, the second derivative of the nozzle radius must be continuous. Although a continuous second derivative can be provided by a series of third-order equations, use of higher-order equations allows coverage of longer nozzle lengths in each equation; thus, fewer equations are needed. In general, the curve fit should allow inflection of the second derivative, and, thus, a series of fifth-order equations is used to curve fit the MOC + BL coordinates. The lengths of the sections were adjusted to provide a good fit of the existing coordinates. Five sections were needed, as shown in Fig. 10.

At the match point between each section, the coefficients were adjusted until there was a match for nozzle radius, slope, and curvature.

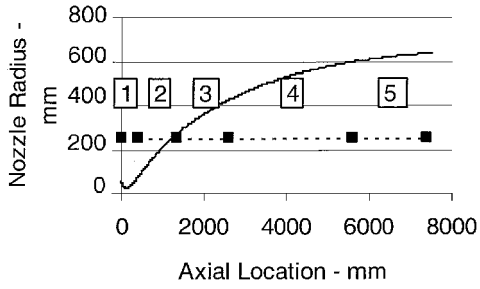

Fig. 10 Sections of nozzle for curve fit procedure.

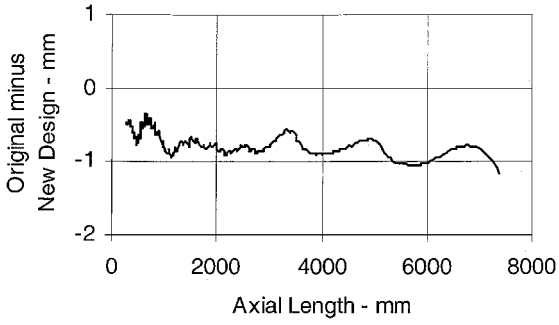

Fig. 11 Comparison of original contour with new contour.

The section from about 2500 to 5500 mm is covered by a single equation. Selection of this critical section of the nozzle is a subtle, but important point; any wave originating in this range goes directly to the core of the test section, without reflection from a wall boundary layer (which may diffuse the effect). That critical section must be a very smooth and is best provided by a single equation.

Furthermore, because the MOC + BL method is step-by-step process that uses assumptions and averages to compute the downstream points, it is possible that the best coordinates might be slightly different than the computed values. Therefore, exact matching of the MOC + BL coordinates was not a priority in this smoothing process. It is more important to have a smooth contour than to exactly match the MOC + BL computed points.

One criterion for this nozzle was that the existing surface had to be machined at least 0.5 mm so that the new contour could be made with confidence. This allowance was needed for the tolerances of machine setup, concentricity, and a full removal of the existing coating. After smoothing the existing coordinates, this criterion was achieved by rotating the smoothed coordinates 0.00016 rad about a point 2000 mm upstream of the throat.

New Contour

The described method was used to generate several nozzle contours that might improve the flow uniformity. Each contour was evaluated using the CFD programs to predict the flow quality.

The final selected contour is shown in Fig. 11. Figure 11 shows the amount of material that was removed from the original nozzle. It shows the slight modification that was applied to the original nozzle. Note that, exclusive of the general downward trend (resulting from the rotation mentioned earlier), the contour change is only about ±0.25 mm. The peaks in the line at about 3400 and 5000 mm indicate compression corners in the original nozzle; these nearly match the origin of waves suggested in Fig. 3. At each of these two locations, the slope is changed by about 1.6/1000 mm (~0.1-deg change of flow direction); this highlights the need to limit the size of slope variations, especially in the compression mode. Note that the sharp compression corner near 700 mm may have also contributed to the problem (after several reflections); for reference see Fig. 8, which shows several strong waves originating in this area. The flow quality of the new contour is shown in Fig. 12. The improvement from the original nozzle can be seen by comparison to Fig. 8. Most of the disturbances from the wall and the flow disturbances in the test section have been eliminated.

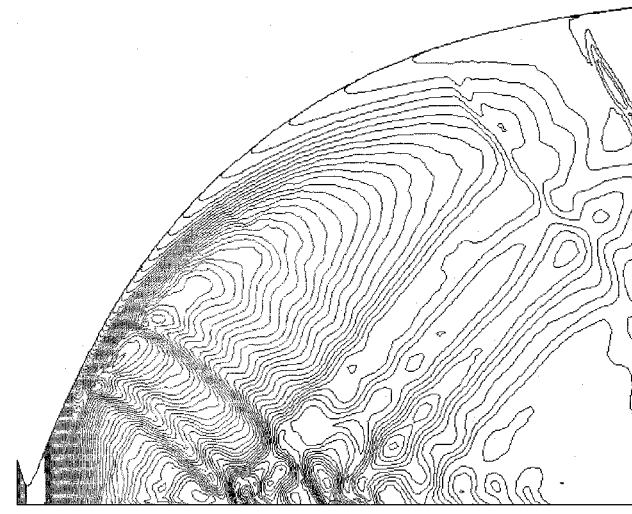

Fig. 12 Flow quality of new contour as designed.

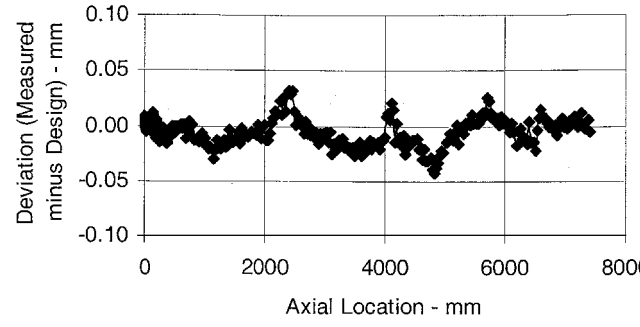

Fig. 13 Results of machining to new contour.

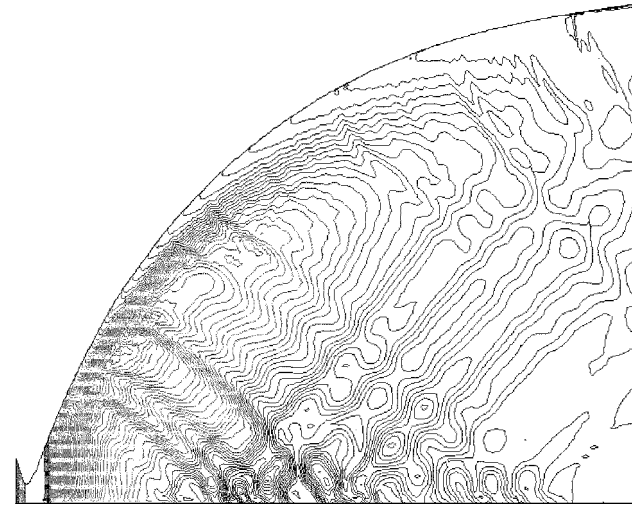

Fig. 14 Flow quality of new contour as machined.

Machining Results

As shown in Fig. 3, the nozzle is in five sections, the throat block and four expansion sections. The throat was replaced; the four expansion sections were remachined using the material of the original nozzle. Each expansion section was too long for a single machine setup; two steps were necessary, one from each end. All measurements were made at about 20°C as a precaution to achieve the design contour. The final finish of electroless nickel was hand polished to 0.8 μm.

The results of the machining to the new contour are shown in Fig. 13. The contour was held to within nearly +,−0.025 mm of the design values. The apparent compression corners near the joints at 2500 and 5800 mm are less than 0.01 deg. There is a step, about 0.03 mm high, near 2500 and a similar gap near 4100 mm. The flow

quality of the nozzle as-machined is predicted as shown in Fig. 14; although there are a few small disturbances in the nozzle, the test section is free from major disturbances.

Test Results

Pitot Pressure

Several improvements were made in the pitot rake before conducting the final tests. The number of pitot probes was increased, and the span was extended so that measurements are at 10-mm transverse spacing and the measurements now extend into the boundary layer. The test data were taken at more axial stations, with 50-mm increments in the axial direction covering 750 mm, in both the horizontal and vertical planes, including tests with off-axis placements (again both in the vertical and horizontal orientations). The data are summarized in Fig. 15. Note that the spread of pitot pressure within the core ± 300 mm around centerline has been reduced from ± 7.5 to $\pm 1.5\%$. The reduced spread of pitot pressure ratio implies that the Mach number variation is now been reduced from ± 1.4 to $\pm 0.3\%$. The tests and data are fully discussed in Ref. 14.

Flow Angle

The flow angularity was measured using a rake with conical probes. The measurements cover 720 mm in width with 7 conical probes spaced 120 mm apart. These tests were made in 10 axial locations, every 100 mm from nozzle exit ($X = 0$) to 900 mm downstream, with the rake in both the vertical and horizontal position, totaling 130 points. With the rake in a horizontal position, the distribution of flow angle was obtained in 7 vertical locations ($z = 0, \pm 0.12, \pm 0.24, \pm 0.3$ m) at 3 longitudinal locations ($x = 0, 0.25$, and 0.5 m), totaling 147 points (some duplicating the longitudinal positions).

The flow inclination angles were from -0.02 to 0.1 deg on the centerline and within ± 0.2 deg in the whole core flow region. An example of the result at the nozzle exit cross section is shown in Fig. 16. The flow is nominally axisymmetric with slight inward flow at this location. Additional information about these tests is included in Ref. 15.

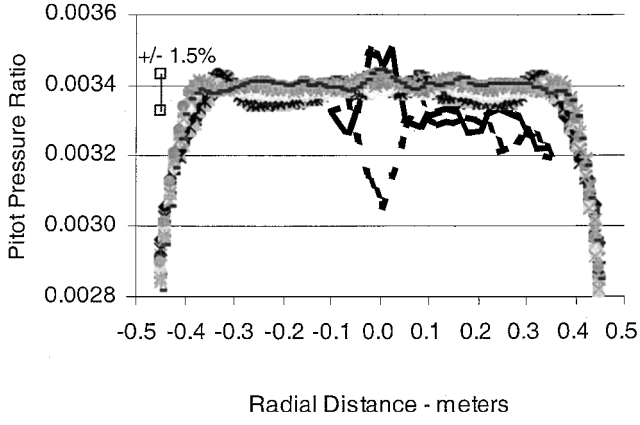

Fig. 15 Final test results summary of test data after modification, original nozzle: – – –, 0 cm and – – –, 75 cm.

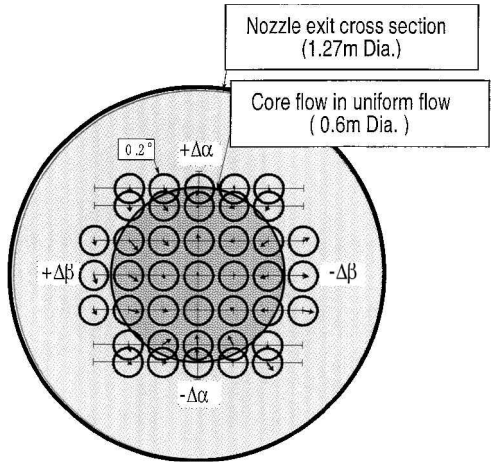

Fig. 16 Flow inclination angle distribution at nozzle exit cross section.

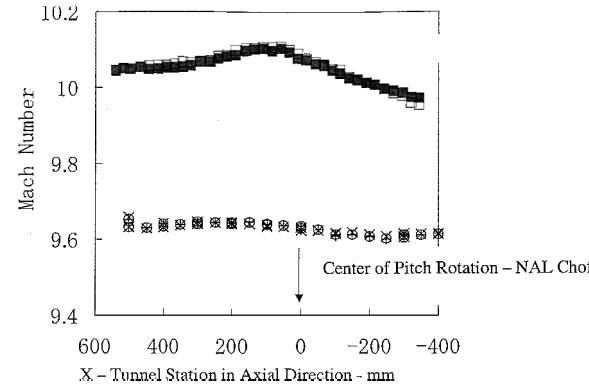

Fig. 17 Centerline Mach number variation, compared with AEDC Tunnel C: ■, AEDC, $Z = -6.4$ mm; □, AEDC, $Z = 6.4$ mm; +, NAL, $Z = -10$ mm; ○, NAL, $Z = 0$ mm; and ×, NAL, $Z = 10$ mm.

Centerline Mach Number

Further evidence of the flow quality achieved in this effort is shown in Fig. 17 (taken from Ref. 16). Figure 17 shows the comparison of the centerline Mach number in this wind tunnel as compared to the same parameter in the Arnold Engineering Development Center Tunnel C. The long length of nearly constant Mach number in the NAL tunnel is apparent.

Conclusions

An international team has studied the flow quality of the NAL Chofu Mach 10 nozzle. The participants used both experimental data and computational methods to identify concerns and to modify the nozzle contour. The results with the new contour show that the flow quality has been significantly improved. As a result, the NAL Mach 10 wind tunnel can now serve the aerodynamic community as a world-class testing facility.

This work demonstrates the use of fine-grid CFD to compute flows for wall contours with small deficiencies as well as to evaluate new possible contours. The work also establishes a basis for continued use of the MOC + BL method of hypersonic nozzle design when used with a suitable smoothing of the contour coordinates as described herein.

Acknowledgments

The authors acknowledge the contributions of Seizo Sakakibara and Koichi Hozumi of the National Aerospace Laboratory, Chofu, who also contributed to the project and this paper.

References

[1] Boudreau, A. H., "Performance and Operational Characteristics of AEDC/VKF Tunnels A, B, and C," Arnold Engineering Development Center, AEDC-TR-80-48, Arnold AFB, TN, July 1981.

[2] Micol, J. R., "Hypersonic Aero-dynamic/Aerothermodynamic Testing Capabilities at Langley Research Center: Aerothermodynamic Facilities Complex," AIAA Paper 95-2107, 1995.

[3] Benton, J., and Perkins, J., "Limitations of the Methods of Characteristics when Applied to Axisymmetric Hypersonic Nozzle Design," AIAA Paper 90-0102, Jan. 1990.

[4] Korte, J. J., "Inviscid Design of Hypersonic Wind Tunnel Nozzles for a Real Gas," AIAA Paper 2000-0677, Jan. 2000.

[5] Aerodynamics Dept., "Plan and Structure of Large-size Hypersonic Wind Tunnel," National Aerospace Lab., TR-1261, Chofu, Tokyo, 1995 (in Japanese).

[6] Fitch, C. R., "Flow Quality Improvement at Mach 8 in the VKF 50-Inch Hypersonic Wind Tunnel B," Arnold Engineering Development Center, AEDC-TR-66-82, Arnold AFB, TN, May 1966.

[7] Hannemann, K., "Numerical Flow Field Analysis of the RWG Mach 6.8 Contoured Nozzle," DLR, German Aerospace Research Center, Rept. IB 223-95 A 46, Goettingen, Germany, May 1996.

[8]Ishizaka, K., Ikohagi, T., and Daiguji, H., "A High Resolution Finite-Difference Scheme for Compressible Gas-Liquid Two Phase Flows," *Proceedings of the 5th ISCFD*, Vol. 1, International Symposium on Computational Fluid Dynamics, Sendai, Japan, 1993, pp. 352–357.

[9]Eggers, A. J., Jr., "One-Dimensional Flows of an Imperfect Diatomic Gas," NACA Rept. 959, 1950.

[10]Ames Research Staff, "Equations, Tables And Charts For Compressible Flow," NACA TR 1135, 1953.

[11]Korte, J. J., Kumar, A., Singh, D. J., and White, J. A., "CAN-DO—CFD-Based Aerodynamic Nozzle Design and Optimization Program for Supersonic/Hypersonic Wind Tunnels," AIAA Paper 92-4009, July 1992.

[12]Korte, J. J., Hedlund, E., and Anandakrishnan, S., "A Comparison of Experimental Data with CFD for the NSWC Hypervelocity Wind Tunnel 9 Mach 14 Nozzle," AIAA Paper 92-4010, July 1992.

[13]Korte, J. J., and Hodge, J. S., "Flow Quality of Hypersonic Wind-Tunnel Nozzles Designed Using Computational Fluid Dynamics," *Journal of Spacecraft and Rockets*, Vol. 32, No. 4, 1995, pp. 569–580.

[14]Sakakibara, S., Sekine, H., Hirabayashi, N., Koyama, T., Tsuda, S., and Nagai, S., "Flow Quality of the NAL 1.27 m Mach 10 Re-machined Nozzle," 43rd Space Science and Technology Conf., Japan Society for Aeronautical and Space Sciences, Paper 99-3E1, Oct. 1999 (in Japanese).

[15]Sekine, H., Tsuda, S., Nagai, S., Koyama, T., Hirabayashi, N., Hozumi, K., and Sakakibara, S., "Flow Characteristics of the NAL Large Hypersonic Wind Tunnel–Flow Inclination Angle Distribution," 44th Space Science and Technology Conf., Japan Society for Aeronautical and Space Sciences, Paper 00-1B11, Oct. 2000 (in Japanese).

[16]Nagai, S., Tsuda, S., Koyama, T., Hirabayashi, N., and Sekine, H., "Comparison of Winged Vehicle Force Data at Large Hypersonic Wind Tunnels," AIAA Paper 2001-0166, Jan. 2001.

T. C. Lin
Associate Editor